Differentiated spring behavior under changing hydrological conditions in an alpine karst aquifer

Maria Filippini [a], Gabriela Squarzoni [a,*], Jo De Waele [a], Adriano Fiorucci [b], Bartolomeo Vigna [b], Barbara Grillo [c,d], Alberto Riva [e,f], Stefano Rossetti [g], Luca Zini [d], Giacomo Casagrande [h], Christine Stumpp [i], Alessandro Gargini [a]

[a] Department of Biological, Geological and Environmental Sciences, Alma Mater Studiorum University of Bologna, via Zamboni 67, 40126 Bologna, Italy
[b] Department of Environment, Land and Infrastructure Engineering, Politecnico di Torino, Corso Duca degli Abruzzi, 24, 10129, Torino, Italy
[c] Pordenone Speleological Union, Pordenone, Italy
[d] Mathematics and Geosciences Department, University of Trieste, via Valerio 12/1, 34127 Trieste, Italy
[e] Department of Physics and Earth Sciences, University of Ferrara, via Savonarola 9, 44100 Ferrara, Italy
[f] Caving Group "Solve" CAI, Belluno, Italy
[g] Ferrarese Speleological Group, via Canal Bianco, 44124 Ferrara, Italy
[h] Autonomous Region of Friuli Venezia Giulia – Integrated Hydrological Service, Water Resources Management and Safeguard of Water from Pollution, via Longarone, 38, 33100 Udine, Italy
[i] Helmholtz Zentrum München, German Research Center for Environmental Health, Institute of Groundwater Ecology, Ingolstädter Landstr. 1, D-85764 Neuherberg, Germany

ARTICLE INFO

Accepted 22 November 2017

Keywords:
Karst hydrogeology
Tracer tests
Chemographs
Hydrographs
Geochemical monitoring

ABSTRACT

Limestone massifs with a high density of dolines form important karst aquifers in most of the Alps, often with groundwater circulating through deep karst conduits and water coming out of closely spaced springs with flow rates of over some cubic meters per second. Although several hydrogeological studies and tracing experiments were carried out in many of these carbonate mountains in the past, the hydrogeology of most of these karst aquifers is still poorly known.

Geological, hydrodynamic and hydrochemical investigations have been carried out in one of the most representative of these areas (Cansiglio-Monte Cavallo, NE Italy) since spring 2015, in order to enhance the knowledge on this important type of aquifer system. Additionally, a cave-to-spring multitracer test was carried out in late spring 2016 by using three different fluorescent tracers. This hydrogeological study allowed: 1) gathering new detailed information on the geological and tectonic structure of such alpine karst plateau; 2) defining discharge rates of the three main springs (Gorgazzo, Santissima, and Molinetto) by constructing rating curves; 3) understanding the discharging behavior of the system with respect to different recharge conditions; 4) better defining the recharge areas of the three springs.

The three nearby springs (the spring front stretches over 5 km), that drain the investigated karst aquifer system, show different behaviors with respect to changing discharge conditions, demonstrating this aquifer to be divided in partially independent drainage systems under low-flow conditions, when their chemistry is clearly differentiated. Under high-flow conditions, waters discharging at all springs show more similar geochemical characteristics. The combination of geochemistry, hydrodynamic monitoring and dye tracing tests has shown that the three springs have different recharge areas. The study points out that even closely spaced karst springs, that apparently drain the same karst mountain, can have different behaviors, and thus distinctive reactions toward polluting events, a characteristic to be taken into account for their management.

1. Introduction

The Alpine chain is characterized by several mountainous karst aquifers, supplying drinkable water to many cities in France, Switzerland, Austria, Italy, and Slovenia (Goldscheider and Neukum, 2010). These aquifers generally have their recharge areas at altitudes above 1000 m asl, and are fed by direct recharge via rainfall, mainly during summer and autumn (July–November), and via snowmelt, mainly during spring (March–June) (Vigna and Banzato, 2015). Discharge often occurs through major springs of magnitude between 1 and 2 (Meinzer, 1923, i.e. 1 m^3/s–>10 m^3/

* Corresponding author.
E-mail address: gabriela.squarzoni2@unibo.it (G. Squarzoni).

s), located at the foot of mountains, and some of these are connected to aqueducts of major cities (e.g. Vienna, Plan et al., 2010). However, such important resources of drinking water are generally poorly exploited (e.g. Turk et al., 2015), and many big cities located in the plain areas surrounding the mountainous karsts still mostly rely upon groundwater abstraction from alluvial aquifers (Zini et al., 2013).

Karst aquifers are also much more vulnerable to pollution than other aquifers (Marín and Andreo, 2015), and this is among the reasons why they are often underexploited, compared to porous aquifers. On the other hand, in the foreseeable future, the use of these carbonate aquifers as a strategic reservoir of high-quality water will become essential in order to manage the expected water shortage crisis induced by global change and overdrafting of groundwater in the main urbanized plains of the world (Liu et al., 2017).

Vulnerability mapping of karst aquifers is a challenging task. Different methods often deliver non-univocal outputs, depending on flow conditions and the intrinsic characteristics of the karst system (Ravbar and Goldscheider, 2009; Wachniew et al., 2016).

Alpine karst aquifers can be broadly classified in three different conceptual underground drainage models (i.e. dominant conduit model, interconnected conduit model, and dispersive circulation model; Vigna and Banzato, 2015), mainly based on their lithological and structural characteristics, their degree of karstification, the geometry of the underground drainage network, and the extension of their phreatic (i.e. saturated) zone. Such characteristics influence the hydrodynamics and physicochemical parameters of the water at the karst springs in response to recharge events:

(1) systems with dominant conduit drainage have a high permeability and a quick response to recharge events. Generally, the phreatic zone is not well developed, and waters tend to flow along a few important and prevalently vadose conduits. Flow rates at the springs of these systems show variations up to two or more orders of magnitude during important infiltration events, and mineralization and temperature change rapidly after a hydrologic recharge event because neoinfiltrating waters arrive quickly; (2) systems with interconnected conduit drainage have well-developed (interconnected) phreatic conduits and a more or less karstified fracture system. This phreatic zone forms an important reservoir, and the excursion of hydraulic head can be huge, up to variations of over 100 m. In this type of system, springs are generally vauclusian (deep phreatic drowned shafts) and show rather significant flow rate changes, but also a longer time of depletion. Increase of flow rates is generally related to hydraulic pressure (not to the neoinfiltrated water), and the water at the spring shows increased temperature and mineralization (piston flow); (3) systems with dispersive circulation are less permeable and karstified, composed of an interconnected network of more or less karstified fractures. These systems do not show preferential drainage routes and are characterized by a thick phreatic zone. Flow rate variations at the springs are subdued and the chemical and physical parameters of the waters coming out of the springs are relatively constant.

A general distinction between different types of karst drainage systems helps addressing vulnerability and pollution risk assessments (Vigna and Banzato, 2015), but these assessments generally require in-depth investigations using a combination of different techniques (Stumpp et al., 2016). Despite broad classifications, karst aquifers are in fact very heterogeneous with triple porosity (i.e. primary matrix porosity, fractures and conduits) (White, 2002; Hartmann et al., 2014). The anisotropy typical of these aquifers makes them difficult to understand fully, and modeling approaches (e.g. KARSYS, Jeannin et al., 2013; Ballesteros et al., 2015; Turk et al., 2015) cannot entirely simulate their storage capacity and hydrodynamic and transport behavior during different flow regimes.

Also, karst aquifers often show different behavior under varying hydrological conditions, depending on the architecture of the aquifer at different altitudes. In the Xiangxi River Basin (South China), for example, during high-flow conditions the springs behave as discharge points of a dominant conduit drainage system, whereas during low-flow conditions the general behavior of the system is more similar to the interconnected conduit drainage model (Luo et al., 2016). In the Julian Alps (Kanin Mountain, on the border between Slovenia and Italy), the general model during low-flow conditions has been reconstructed based on monitoring and tracer test data. However, it is known that overflows between the different karst compartments occur during high-flow condition. This last condition is not well understood yet, because of the lack of specific data (e.g. tracing experiments during floods) (Turk et al., 2015). In the Wetterstein Mountains (Germany), an interconnection between adjacent karst compartments has also been observed during high-flow conditions by means of natural and artificial tracers (Lauber and Goldscheider, 2014). During high-flow conditions, the chemical properties of the outflowing waters in adjacent springs that drain the same karst aquifer can show homogenization, as the case of the Lička Jesenica river, fed by the two springs Malo and Veliko Vrelo (Terzić et al., 2012). In some other cases, high-flow conditions cause the catchment areas of the springs to increase, leading to variations in water chemistry, if the increased hydrogeologic watershed involves areas with different lithologies (e.g. the Aubonne karst catchment area, in the Swiss Jura) (Ravbar et al., 2011; Perrin and Luetscher, 2008).

Only a combination of artificial and natural tracer tests under different flow conditions can help unraveling this complexity. Artificial tracers reveal the groundwater flow pattern through the conduit and karstified fracture system, the flow velocity and storage distribution and the dispersivity. On the other hand, natural tracers can provide insight into the provenance of the resident waters pushed out of the aquifer by the hydraulic pressure, and into the time of neo-infiltrated water arrival or average altitudes of recharge areas.

Concerning the carbonate massifs in the Southern Alps, these are often drained by springs of high discharge, generally related to a low permeability threshold. Some of these springs, in the terminal sector of the groundwater flow system, consist of deep flooded shafts that have been explored by cave divers up to depth greater than 200 m bgs (below ground surface). The recharge areas of these springs are generally reconstructed on the basis of detailed geological, geomorphological, and structural mapping, and by means of tracer tests (Perrin and Luetscher, 2008; Kuebeck et al., 2013; Lauber and Goldscheider, 2014). However, since most of the time the drainage network feeding these springs is only partially known, essential information on the aquifer architecture is to be searched in the spring flow dynamics and hydrochemical monitoring (Panagopoulos and Lambrakis, 2006; Ravbar et al., 2011, Terzić et al., 2012).

This paper reports the study of a complex karst area (Cansiglio-Monte Cavallo, NE Italy) that hosts one of the most representative carbonate aquifer systems in the Southern Alps. Three main springs are located along a resurgence front of over 5 km, draining the same carbonate mountain aquifer (Fig. 1). Geological, geomorphological, and structural analyses, hydrochemical monitoring of springs, chemical analyses of waters, flow rate measurements and a multitracer test have allowed highlighting the different behavior of such springs under changing hydrological conditions, emphasizing the complexity of this aquifer system.

2. Study area

The Cansiglio-Monte Cavallo karst area is located at the border area between the Veneto and Friuli-Venezia Giulia regions, in northeastern Italy (Fig. 1). This area lies in the southwestern most

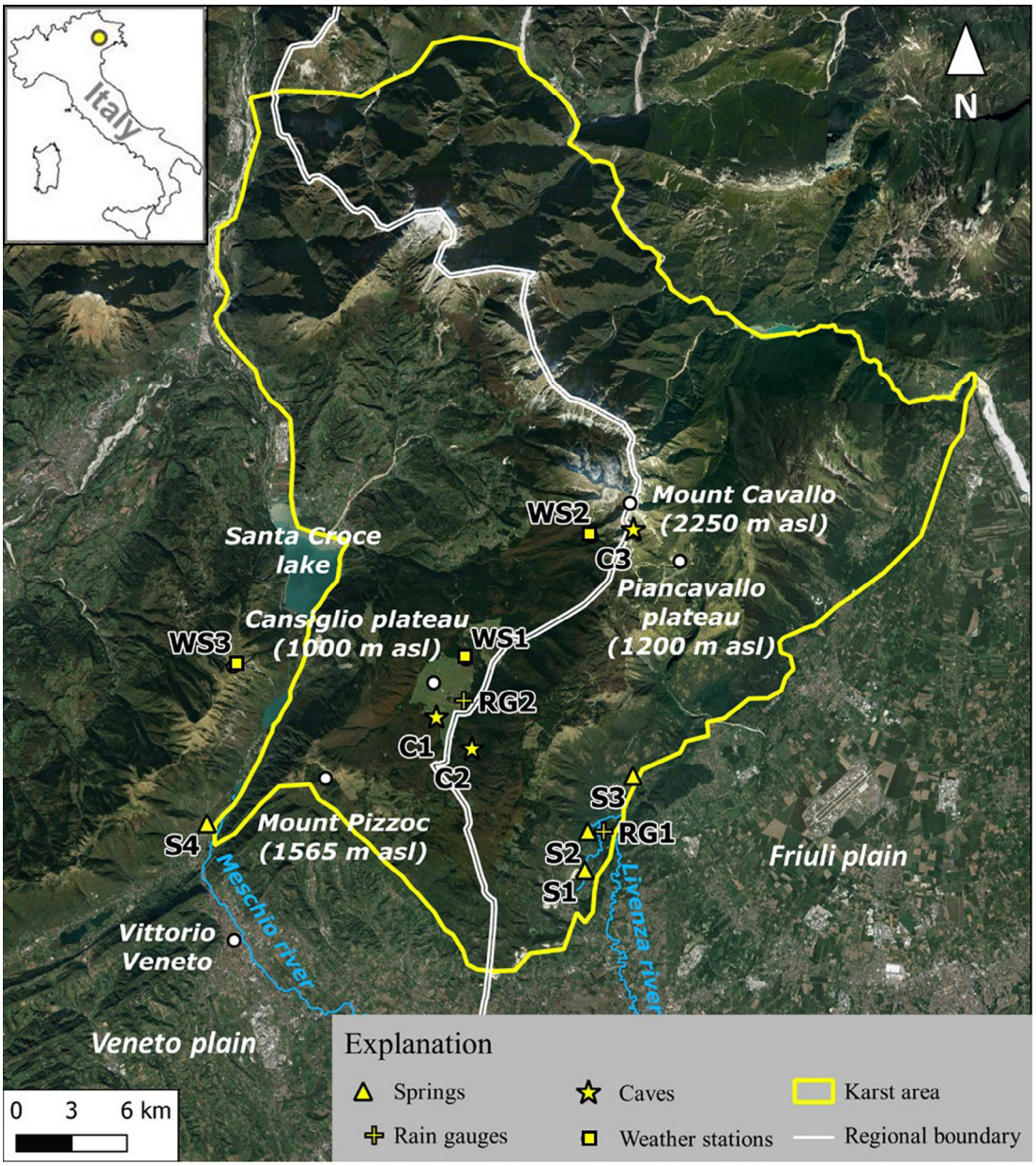

Fig. 1. Location of the Cansiglio-Monte Cavallo karst aquifer system. The boundaries of the karst area correspond to contacts between the carbonate rocks and the adjacent less permeable units and/or to regional fault structures.

part of the Carnian Alps and is bordered by the Cellina valley to the north, by the Santa Croce lake to the west, and by the Veneto and Friuli plains to the south and east. The study area can roughly be divided into two plateaus, Cansiglio and Piancavallo, located at 1000 and 1200 m asl, respectively, and the Cavallo mountain chain attaining the highest altitude at 2250 m asl. At the southeastern border, along the contact with the plains, three springs drain the aquifer system, from north to south: Gorgazzo ("S3" from now on, 45 m asl), Santissima ("S2", 32 m asl), and Molinetto ("S1", 28 m asl) (Fig. 2). This group of springs represents, in terms of total spring-flow (8 m^3/s on average), the second largest location of groundwater discharge throughout the whole Alps after the spring of the Timavo river in the Gulf of Trieste (northern Adriatic sea) that has a discharge of about 30 m^3/s (Civita et al., 1995; Zini et al., 2014). The three springs represent a valuable and easily accessible resource for drinkable water and other economic activities (e.g. fish farming) and give birth to the Livenza river that flows southward toward the Adriatic sea. Another major spring (i.e. Meschio, "S4") is located near Vittorio Veneto, at the southwestern border of the Cansiglio massif, but probably discharges from a separate karstic groundwater flow system and hydrogeologic watershed that corresponds to the western flank of the Meschio river (Fadalto valley).

Geologically, the massif is mainly composed of carbonate rocks ranging in age from Upper Triassic to Miocene (Cavallin, 1979). These were deposited in a variety of marine environments, from the deep sea to the continental slope and platform, including back-, fore- and inner-reef settings (Fig. 3). The oldest rocks are the dolostones and dolomitic limestones of the Triassic Dolomia principale Formation, outcropping only in the northern most part of the study area, followed by a thick sequence of different types of limestone with ages ranging from lower Jurassic to upper Cretaceous (Cancian et al., 1985). The massif is bounded on almost all sides by regional thrust faults. The three main springs are aligned

Fig. 2. The three main springs investigated: A) Molinetto ("S1"), B) Santissima ("S2") and C) Gorgazzo ("S3").

along a NNE-SSW front of over 5 km corresponding to a fault on the southwestern border of massif, known as the Caneva-Maniago line that puts in contact the Jurassic-Cretaceous limestones with the Tertiary and Quaternary less permeable units to the east (Section A-A′ in Fig. 3). These last units work as a low permeability threshold forcing groundwater outflow. The general structure of the massif is that of a gently folded succession, with an asymmetric NNE-SSW oriented anticline in the eastern part, followed by a wide syncline structure to the west on which the Cansiglio plateau is developed. The main fracture system is oriented NW-SE, followed by sets with a NNE-SSW direction (Vincenzi et al., 2011).

The massif is dotted with dolines, especially numerous in its southeastern portion where pure limestones predominate (Cucchi and Finocchiaro, 2017). Surface drainage is almost completely absent, except where local patches of less permeable material cover the carbonate rocks. Although over 200 caves have been explored on the massif, no important underground rivers have been identified so far. The most interesting caves, with some perennial water flow along their galleries, are known as Bus de la Genziana ("C1" from now on), Abisso Col della Rizza ("C2"), and Fessura della Tosca ("C3") (Fig. 1). The first (C1) is an alpine abyss opening at 1020 m asl and almost 600 m deep, developed along vadose shafts giving access to a series of underground canyons in which small rivers flow in different directions. C2 is the deepest cave on the Cansiglio plateau (almost 800 m) opening at 1115 m asl and reaching 320 m asl at its deepest explored point. This cave hosts a small river that has carved an underground narrow canyon. C3, instead, is a modest vertical cave opening at 1885 m asl, around 250 m deep and with a perennial subterranean stream of a few L/s. None of these caves reaches the phreatic zone, and all are typically vadose shafts and canyons.

Among the major springs, S3 and S4 have been explored by cave divers (Fig. 4). S4 opens at 200 m asl on the right side of the Meschio river which flows at around 165 m asl, almost 20 m below the deepest explored drowned conduit in the spring (this last one being explored down to 185 m asl; Fig. 4B). Geological and morphological evidence (dip of the carbonate beds, presence of NNE-SSW lineaments) suggest the western flank of the Meschio river to be the most probable recharge area of this spring, although recharge from the Cansiglio plateau cannot be completely excluded. This spring appears thus to be draining the carbonate aquifer located to the West of Cansiglio plateau.

On the other hand, the S3 spring is the most downstream source of the Livenza river and is located at 45 m asl. The main phreatic conduit of S3 has been explored by Luigi Casati down to a depth of 212 m bgs (167 m bsl). In recent explorations an additional conduit has been discovered at around sea level, developing more or less horizontally in a westward direction (Luigi Casati, personal communication).

The three main springs were studied in the past for their flow rates and chemistry and it turned out that the biggest one (S2) is recharged from higher altitudes compared to S1 and S3 (Cucchi et al., 1999; Grillo, 2007). The discovery of some active groundwater flow in the C2 cave allowed Vincenzi et al. (2011) to carry out a first multiple dye tracing experiment in 2008, injecting 10 kg of Tinopal-CBS-X in C1 cave at 100 m depth (920 m asl) along the main underground river, and 5 kg of Uranine in C2 cave at 250 m depth (at a slightly lower altitude of injection point in C1). Uranine was found in both S1 and S2 springs but not in S3. Tinopal-CBS-X was not detected and no other connections were ascertained.

Grillo et al. (2011) and Devoti et al. (2015) investigated slope deformations in the Cansiglio massif by means of a geodetic survey into caves. The authors infer that the observed deformations are hydrologically induced suggesting fast and impulsive response of the karst hydrologic system to the main recharge events. The main deformation direction is towards the Livenza springs (S1, S2 and S3) that appear to be the main discharge points of the aquifer system. All these studies were the starting point of our investigations.

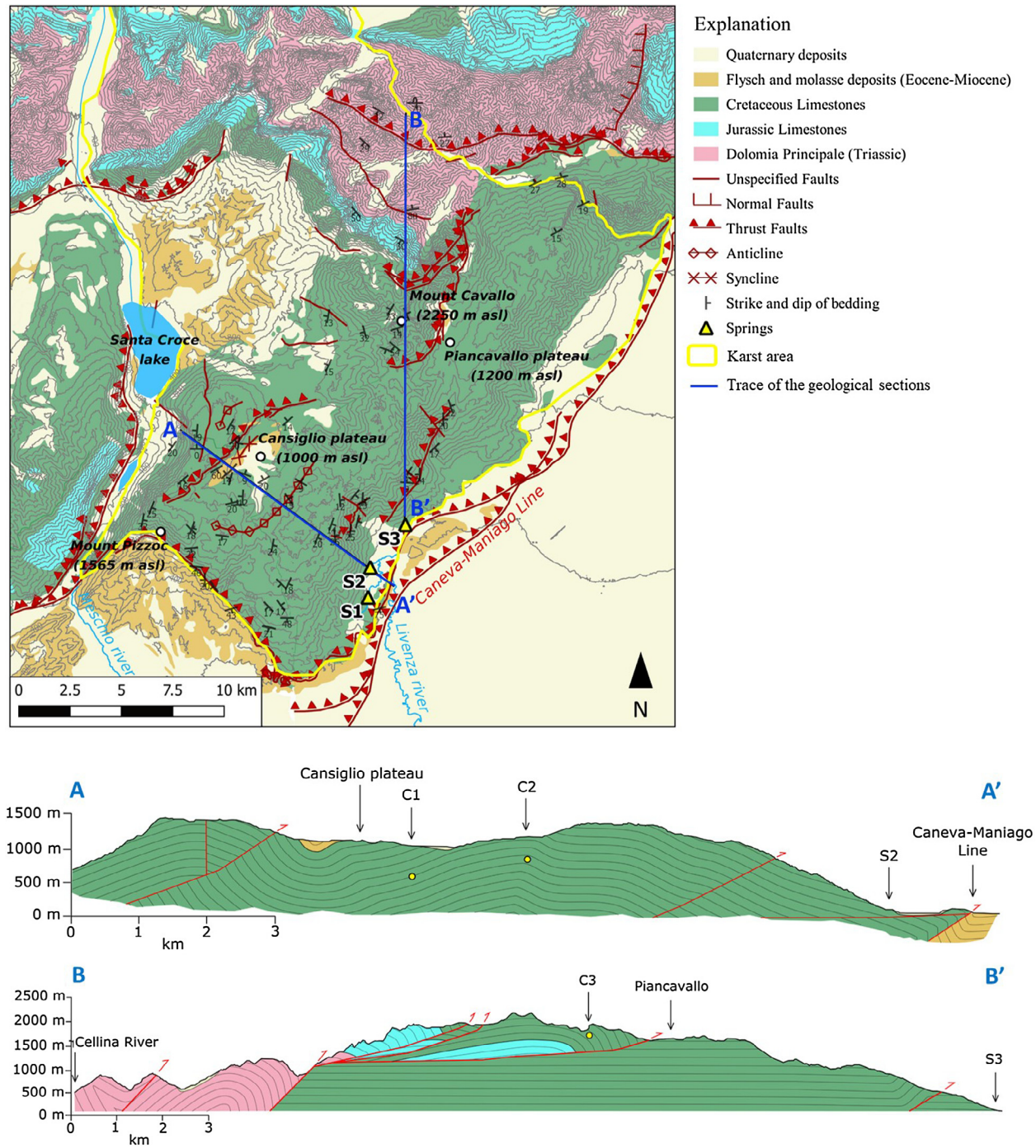

Fig. 3. Geological sketch map of the Cansiglio-Monte Cavallo karst aquifer (above) and representative geological sections (below); the yellow dots on the geological sections show the depth of tracer injection in the C1, C2 and C3 caves.

3. Material and methods

3.1. Lineament survey

Main lineaments and geological boundaries were surveyed using SRTM (Shuttle Radar Topography Mission) images, and combined and compared with the data obtained from Landsat images by Vincenzi et al. (2011). Data were analyzed using the Dips application (Rocscience ©). Terrain surveys were carried out in some areas for a field check of the major lineaments.

3.2. Climate data

Air temperature, rainfall and snow cover data were obtained from the Meteorological and Snow and Avalanches Service of the Regional Authority for the Protection of the Environment of Veneto region (ARPAV). The weather station considered for hourly rainfall and hourly air temperature was Cansiglio-Tramedere ("WS1", 1028 m asl); the stations considered for hourly snow cover thickness were Casera Palatina ("WS2", 1505 m asl) and Faverghera ("WS3", 1605 m asl) (Fig. 1). The snow cover data are shown in the Supplemental Material.

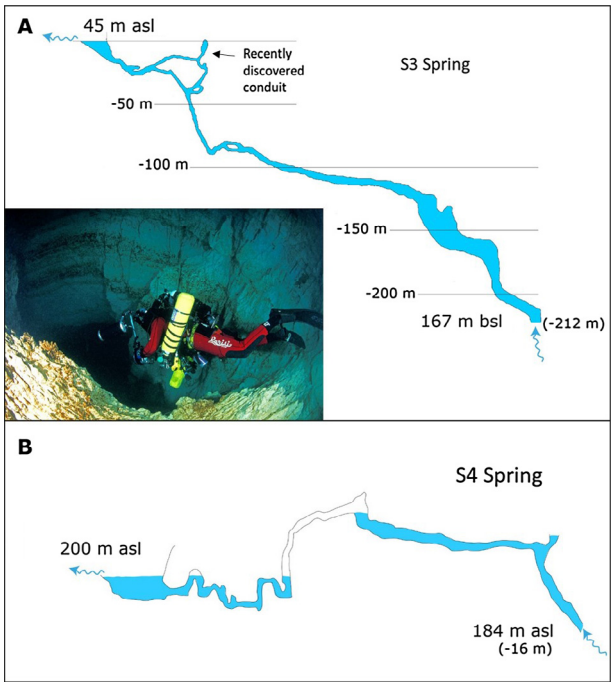

Fig. 4. The two explored karst springs at the foot of the Cansiglio plateau. A: S3 spring (survey by Jean Jacques Bolanz and Luigi Casati; photo of the vertical drowned shaft by Roberto Rinaldi); B: S4 spring (survey by Gruppo Grotte Treviso).

3.3. Flow rate measurements

In order to reconstruct a rating curve for the springs, a series of direct measurements of spring total flow rates (Q) were carried out in different discharge conditions (see details in the Supp. Mat.). At S3 spring these measurements were carried out in the streambed immediately downstream of the discharge point, using an Acoustic Doppler Velocimeter (Flowtracker, SonTek/YSI Inc). At S1 and S2 an Acoustic Doppler Current Profiler (StreamPro, Teledyne RD Instruments ©) installed on a remote controlled vessel was used, because of the higher flow rate and the impossibility of fording the riverbed.

3.4. Hydrological and T/EC monitoring

The stage of three main springs at the outlet (h), along with water temperature (T) and specific electrical conductivity (EC) at 25 °C, have continuously been monitored, every 30 min (S1 and S3) and hourly (S2), from February 20th 2015 (S2) or March 25th 2015 (S1 and S3) to August 29th 2016. The monitoring period included extreme hydrological events (floods and dry periods) and recharge from snowmelt and rainfall. Multiparametric loggers (CTD-Diver, Schlumberger Water Services ©) have been installed at the spring outlet, while a barometer (Baro-Diver, Schlumberger Water Services ©) was placed close to the S3 spring for barometric correction. Before the monitoring started, the loggers were first placed together at the S2 spring, for a few weeks, to allow data comparison and calibration. Because of works in the streambed close to the outlet of S3 spring, the diver location was changed during the monitoring period.

3.5. Hydrochemistry and water isotopes

3.5.1. Sampling

Groundwater sampling was performed at the 3 springs in 7 different sampling rounds between February and September 2015 to analyze major ions, Rare Earth Elements (mainly Lanthanoids), and water stable isotopes (details on the sampling rounds are reported in the Supplementary Material). Two rain gauges were installed at different altitudes (31 and 1025 m asl) within the study area in order to collect rainwater for water isotope analyses ("RG1" and "RG2" in Fig. 1, respectively).

Samples for hydrochemical analyses of major ions and Lanthanoids were taken as 500 mL of untreated water and 100 mL of acidified water (HNO_3 to pH < 2). Samples for water isotope analyses (including samples from rain gauges) were collected in 8 mL glass vials.

3.5.2. Laboratory analysis

Major ions and Lanthanoids were analyzed at the chemical laboratory of hydrogeological research at the Polytechnic University of Turin. Ca^{2+}, Mg^{2+} and HCO_3^- were obtained by titration, SO_4^{2-}, Cl^- and NO^{3-} were analyzed by Ion Chromatography, K^+ and Na^+ by Atomic Absorption Spectroscopy (AAS), whereas Lanthanoids were analyzed with Inductively Coupled Plasma-Mass Spectrometry (ICP-MS).

Water stable isotopes were analyzed at the Helmholtz Zentrum München by laser-based isotope analysis (L2120-i, Picarro Inc, Santa Clara, USA) relative to Vienna Standard Mean Ocean Water (VSMOW) with a precision of ± 0.1 ‰ for $\delta^{18}O$ and ± 0.5 ‰ for δ^2H.

3.6. Artificial tracer experiments

3.6.1. Tracer injection

Three artificial tracers were used simultaneously for the tracer test: Uranine (sodium Fluoresceine; CAS 518-47-8), Aminorhodamine-G (CAS 5873-16-5), and Tinopal CBS-X (CAS 27344-41-8). 10 kg of Uranine were injected in C1 cave, at an altitude of around 600 m asl (400 m below cave entrance), in a deeper point with respect to the injection performed by Vincenzi et al. (2011) in the same cave, but believed to be along the same underground river. The water discharge at this depth is usually higher allowing an easier operation of tracer injection. The tracer was diluted on May 28th, 2016 with local flow rate in the underground river of around 10 L/s. 5 kg of Aminorhodamine-G were injected in the same spot as for the previous dye tracing experiment (Vincenzi et al., 2011) in the underground stream in C2 at around 850 m asl (250 m below cave entrance), on May 21st, 2016, with local flow rate around 1–2 L/s. Finally, 10 kg of Tinopal CBS-X were injected in C3 at around 1700 m asl (200 m below cave entrance), on June 19th, 2016 (after snowmelt) with local subsurface flow rate in the underground river of around 10 L/s. A detailed timeline of tracer injection is reported in the Supplemental Material. Due to the impossibility of carrying heavy and large volumes of predissolved tracer into the caves, three different teams of speleologists transported the dye powder to the injection points and slowly dissolved it on site. The whole operations lasted 10–12 h for each of the three injections.

3.6.2. Tracer analysis

Tracer arrivals were monitored with three G-GUN field fluorometers (Schnegg and Costa, 2003) installed at S1, S2 and S3 springs (measurements every 15 min). Moreover, three charcoal and three cotton bags were placed in the three springs; a bag of each type remained for the entire period (from April 28th until August 26th, 2016), while the other two bags of each type were replaced every week in a consequential manner. The monitoring period lasted from a week before the first dye tracer injection until 10 weeks after the last injection. One charcoal and one cotton bags were also placed in the S4 spring for the entire monitoring period.

Charcoal bags were analyzed in two independent laboratories (University of Bologna and Polytechnic University of Turin) using

the method described by Vigna (2010). These analyses allowed detecting both Uranine and Aminorhodamine-G. Cotton bags were analyzed using the method described by Vigna (2010) and allowed to detect the presence of Tinopal CBS-X.

4. Results

4.1. Lineament analysis

The analysis of satellite images pointed out the main lineaments, with a predominance of NW-SE and, subordinately, NNE-SSW directions (Fig. 5). The first direction connects some of the major cave systems of the Cansiglio plateau (C1, C2) with two of the main springs (S1 and S2), while the second direction ideally connects the C3 cave with S3 spring.

4.2. Hydrographs

Rating curves were built for the three major springs based on the h/Q discrete monitoring. The single measurements of flow rate and the rating curves are reported in the Supplemental Material. The curves allowed converting the water levels monitored continuously with Divers into flow rates. At the S3 spring, where the Diver was moved to river sections of different geometry during the monitoring period, different rating curves were built for each interval corresponding to the different Diver locations. Maximum, minimum and mean flow rates detected at S1, S2 and S3 are reported in Table 1 together with the discharge Variability ("V", defined as the ratio of discharge fluctuation, i.e. max – min, to the average discharge; Meinzer, 1923). It is worth noting that S3 went totally dry during low recharge periods.

The three springs show a different hydrological behavior (Table 1, Fig.6): S2 has the highest mean flow rate, followed by S3 and S1; S1 and S2 have a lower V with respect to S3. The highest flow rates variations at S3 occur when snowmelt contributes to the recharge ("snowmelt hydroperiod" from now on, extended from March until June), whereas S2 has stronger flow rate variations in response to the intense rainfall ("heavy rainfall hydroperiod" from now on, extended from September until November). Discharge Variability at S1 is similar during the snowmelt and heavy rain hydroperiods. It is worth pointing out that during regular discharge periods the highest amount of water flows out from S2, whereas the highest flow during floods is registered at S3.

4.3. Chemographs

The different behavior of the three springs is also evident from the temporal pattern of physico-chemical parameters (T and EC).

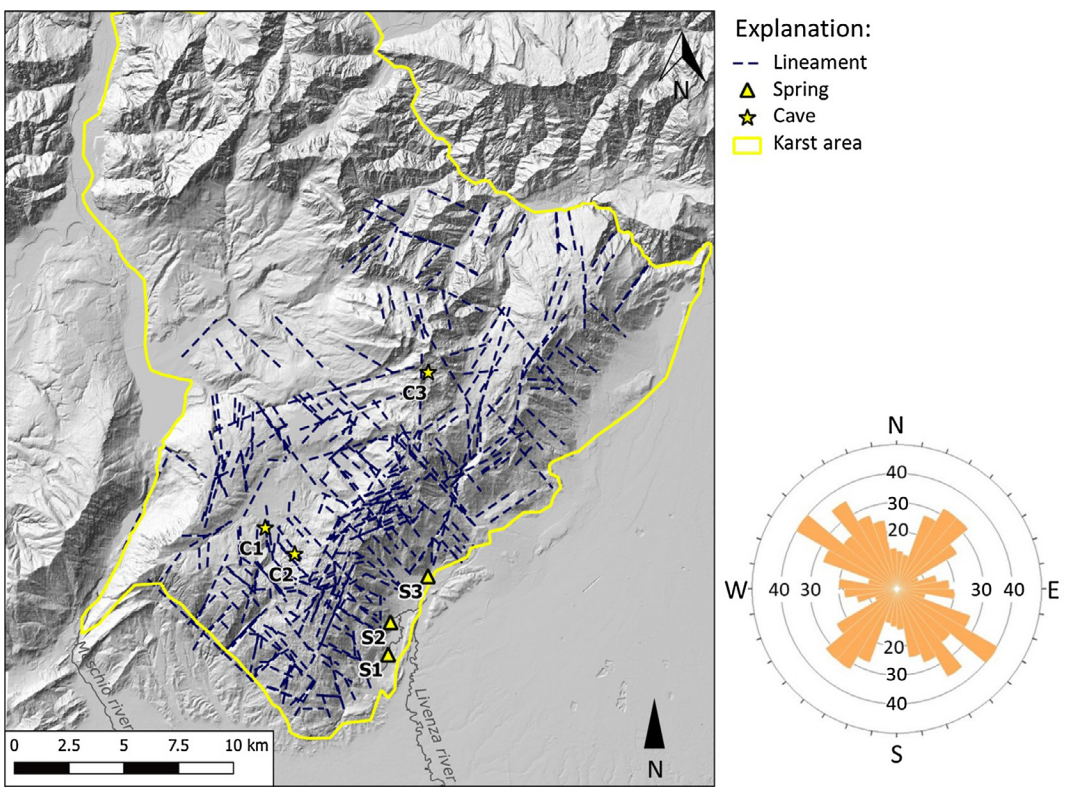

Fig. 5. Lineament map of the Cansiglio karst area as derived from image analysis. The numbers on the rose diagram correspond to the number of lineaments falling in the same class of directions.

Table 1
Maximum, minimum and mean discharge detected at the three springs during the entire monitoring period (March 2015–August 2016). "V" is the discharge Variability during the entire period, defined as in Meinzer (1923). "V snowmelt" and "V rainfall" are the discharge Variabilities corresponding to a snowmelt hydroperiod (March–June 2016) and a heavy rainfall hydroperiod (September–November 2015), respectively.

	Max Q [m^3/s]	Min Q [m^3/s]	Mean Q [m^3/s]	V	V snowmelt	V rainfall
S1	5.1	0.2	1.9	2.5	2.5	2.5
S2	9.9	3.3	5.8	1.1	0.7	0.9
S3	17.6	0.0	3.0	5.8	2.7	2.1

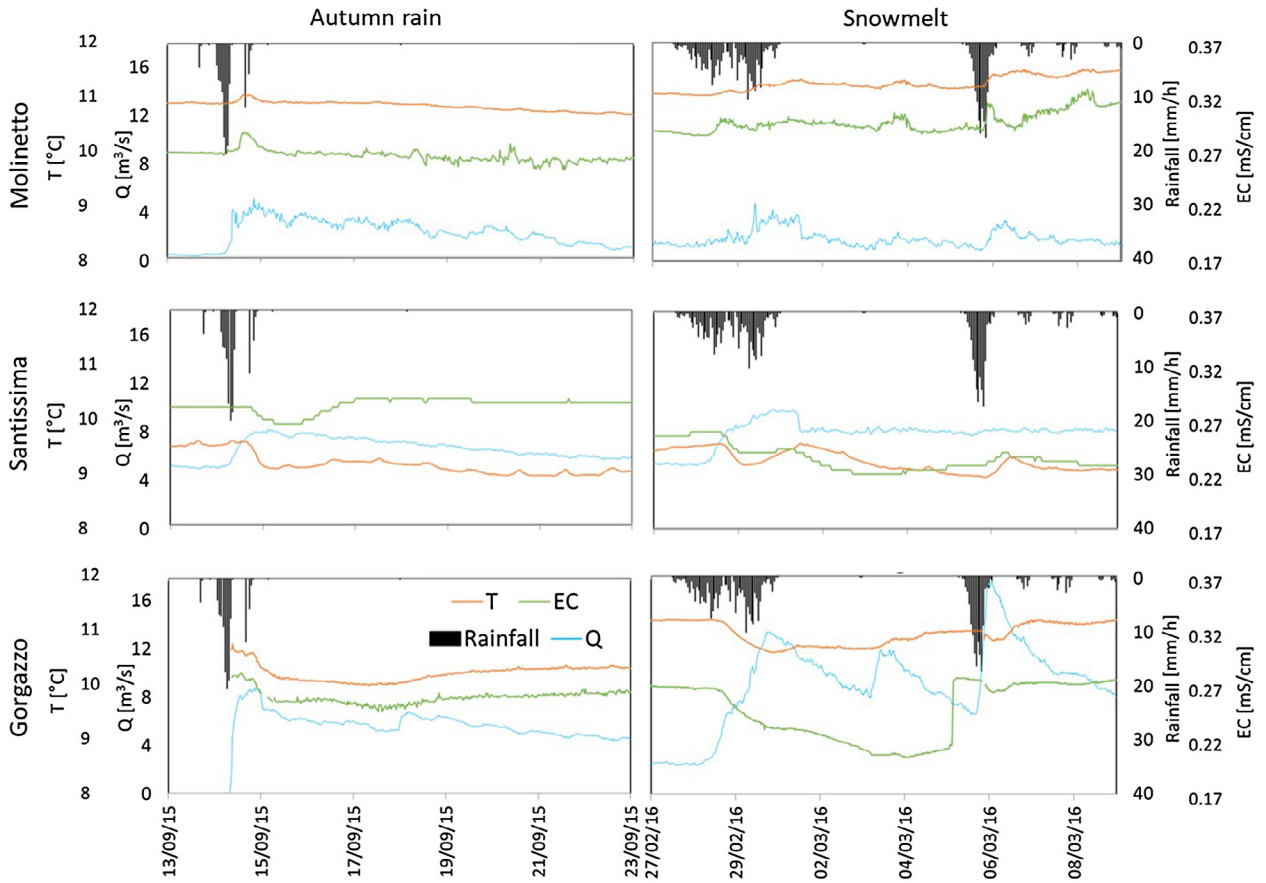

Fig. 6. Detailed response of Q, T and EC to heavy rain (beginning of a heavy rainfall hydroperiod depicted on the left) and to snowmelt (beginning of a snowmelt hydroperiod depicted on the right)) at the three springs (hourly measurements).

Table 2
Maximum, minimum and mean Temperature and Electric Conductivity detected at the three springs during the entire monitoring period (March 2015–August 2016).

	Max T [°C]	Min T [°C]	Mean T [°C]	Max EC [mS/cm]	Min EC [mS/cm]	Mean EC [mS/cm]
S1	11.56	10.49	10.90	0.33	0.23	0.27
S2	9.62	8.61	9.14	0.30	0.22	0.25
S3	11.50	9.75	10.48	0.36	0.17	0.26

The most striking difference is the temperature registered at S2 spring, 1–2 °C lower than in the other two springs (Table 2; Fig. 6). In general, variations in temperature and EC at S1 and S2 are more subdued than in S3 spring, especially during the snowmelt hydroperiod. When analyzing the spring response to recharge events, only S1 appears to register a piston flow phenomenon (with an increase in temperature up to 0.2 °C), confirmed by the subtle increase in EC (up to 0.02 mS/cm) (Fig. 6). The two other springs register a temperature and EC decrease after the main recharge events, with T decreasing by max 0.4 °C and 0.6 °C at S2 and S3, respectively, and EC decreasing by max 0.02 mS/cm and 0.04 mS/cm at the same springs.

4.4. Hydrochemistry of waters at different flow rates

The three investigated springs show the same overall hydrofacies (major elements), with slight differences over time (Fig. 7 and Supp. Mat.). Generally, the first snowmelt recharge (snowmelt hydroperiod, sampling round 2 in Fig. 7) is more mineralized than the recharge induced by late summer-early autumn thunderstorms (heavy rainfall hydroperiod, sampling round 6 in Fig. 7). In particular, Mg^{2+}, Cl^{-}, SO_4^{2-}, and NO_3^{-} are less abundant during the rainfall hydroperiod. The chemical behavior of the three springs is similar in the two sampling rounds (2 and 6) that represent the two main recharge hydroperiods, while it gets different in early summer (sampling round 5), between the two recharge periods, especially for Mg^{2+}, K^{+}+Na^{+}, and Cl^{-}.

It is worth mentioning that Mg^{2+} content is always slightly higher in S3, with a greater difference during periods of normal flow (Δ = 3 mg/L in sampling round 5), the waters getting much more similar during the two recharge hydroperiods (averaged Δ = 1 mg/L in sampling rounds 2 and 6). Mg^{2+} content in S4 (based on one analysis) is higher than in the other springs, and suggests this spring to be fed by the western slopes of the Meschio River (where dolostones are more abundant).

The Lanthanoid contents show a rather subdued but typical fingerprint of waters that have flown in contact with carbonate rocks, with low values in cerium and a higher value in europium (Johannesson et al., 1997a,b; Lee et al., 2003; Nagarajan et al., 2011) (Fig. 8). This carbonate fingerprint appears to be less evident after a significant recharge event (sample 2b in Fig.8), with an increase in all the Lanthanoids and a flattening of the curve, visible especially in S2 and S1. This would indicate a rapid substitution in the conduit system by newly infiltrating waters. Under normal

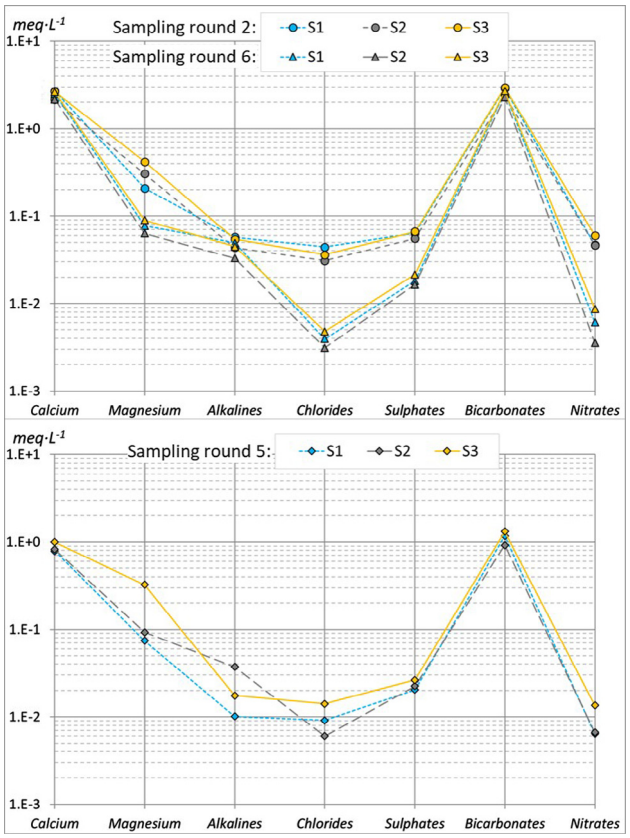

Fig. 7. Schoeller diagram of the three springs after the first snowmelt (snowmelt hydroperiod, sampling round 2) and the first important autumn rains (heavy rain hydroperiod; sampling round 6) (above), and the chemical behavior in between the two recharge hydroperiods (late spring-early summer; sampling round 5). Details on the sampling rounds and measured values are in the Supplementary Material.

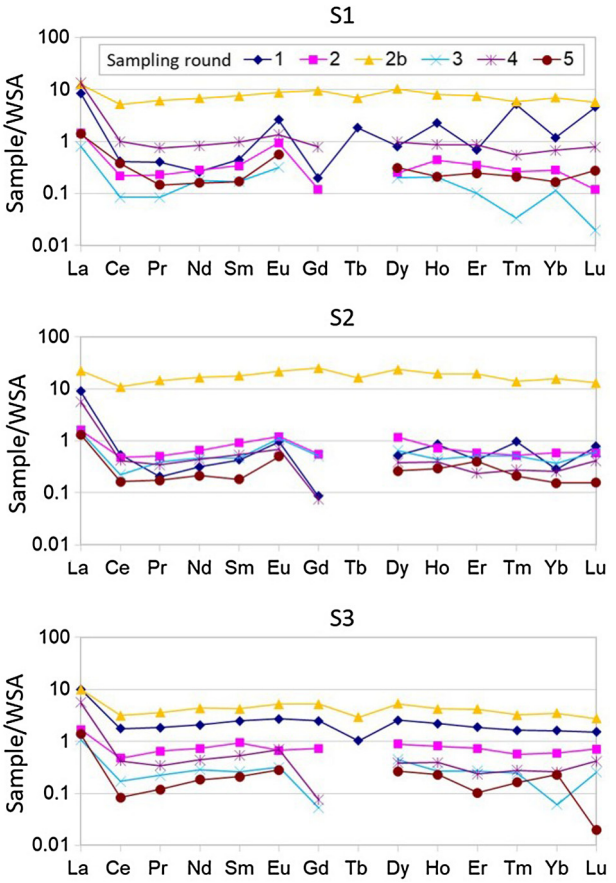

Fig. 8. Lanthanoid concentrations in the three main springs relative to different sampling rounds (concentration on sample normalized on the World Shale Average values; Piper, 1974 – reported in the Supp. Mat.). Details on the sampling rounds and measured values are in the Supplementary Material.

flow conditions, the S3 waters seem to have the least evident carbonate fingerprint (Eu and Ce peaks are almost absent), whereas S1 waters have the most evident Eu and Ce peaks.

All water stable isotope values collected in the study area (rain, spring and cave waters) settle on the meteoric water line for Northern Italian waters (Longinelli and Selmo, 2003). The results of a detailed snow sampling performed by Dietermann and Weiler (2013) in the eastern Alps during snowmelt (Taschinasbach catchment, Switzerland, 1000–2500 m asl) are reported in Fig. 9A as an indication of the snowmelt end-member. Rainwaters have the most enriched isotope ratios, followed by springs, caves, and eventually snow isotopes from the literature (Fig. 9A). S2 shows less enriched stable isotope values compared to the other two springs (Fig. 9B) indicating recharge from higher elevations. The estimation for the differential elevation of the recharge area would be around 350 m, considering an average N-Italian altitude gradient of 0.21‰ per 100 m for $\delta^{18}O$ (considering precipitation stations 1–9 in Longinelli and Selmo, 2003). Spring water sampled during the snowmelt hydroperiod shows pronounced lower values for S2 and S3 (third sampling in Fig. 9B), suggesting a mixing between the rainfall and snow end-members. S1 denotes a much smaller variability in stable isotope composition.

4.5. Artificial tracer test results

Uranine was detected at the S2 spring 4 days after tracer injection and reached a concentration peak of 2.2 μg/L 6 days after injection (Fig. 10). Between the injection and the first tracer arrival, significant rainfall events were registered at the WS1 station, up to 48 mm/day. A second concentration peak (1.3 μg/L) was detected 8 days after tracer injection. A third peak (0.4 μg/L) was detected 15 days after injection, preceded by new significant rainfall events (up to 18 mm/day). Tracer recovery was high, around 75%. Groundwater flow velocity was estimated equal to 1768 m/day, based on the 3D distance between C1 cave and S2 spring (7 km) and the time lag between tracer injection and first arrival. It has to be noted though that such flow velocity only represents the fast response accentuated by the significant recharge events, neglects dispersion and thus is not equal to the average water flow velocity. The estimated flow velocity is 4.6 times higher than the maximum one determined by Vincenzi et al. (2011) for the same aquifer. One possible explanation for this is that no significant precipitation occurred between tracer injection and first arrival in the former tracer test. It is worth noting, however, that the Uranine peak detected by Vincenzi et al. (2011) is similar to the third one observed in the present tracer test ("Peak III" in Fig. 10), both in terms of time lag and concentration. This likely represents a "slower" flowpath that was active in both tracer tests. The results from charcoal bags confirmed the reliability of the curve detected with the fluorometer. These results clearly indicate a connection between C1 cave and S2 spring, which not only consists of one main flow channel but several as indicated by the multiple peaks of the tracer concentration curve.

No other clearly positive charcoal or cotton bags for all tracers were retrieved from all the other springs (including the S4).

The Aminorhodamine-G and Tinopal CBS-X returned no reliable signal at S2, both via fluorometers and charcoal bags. Similar dis-

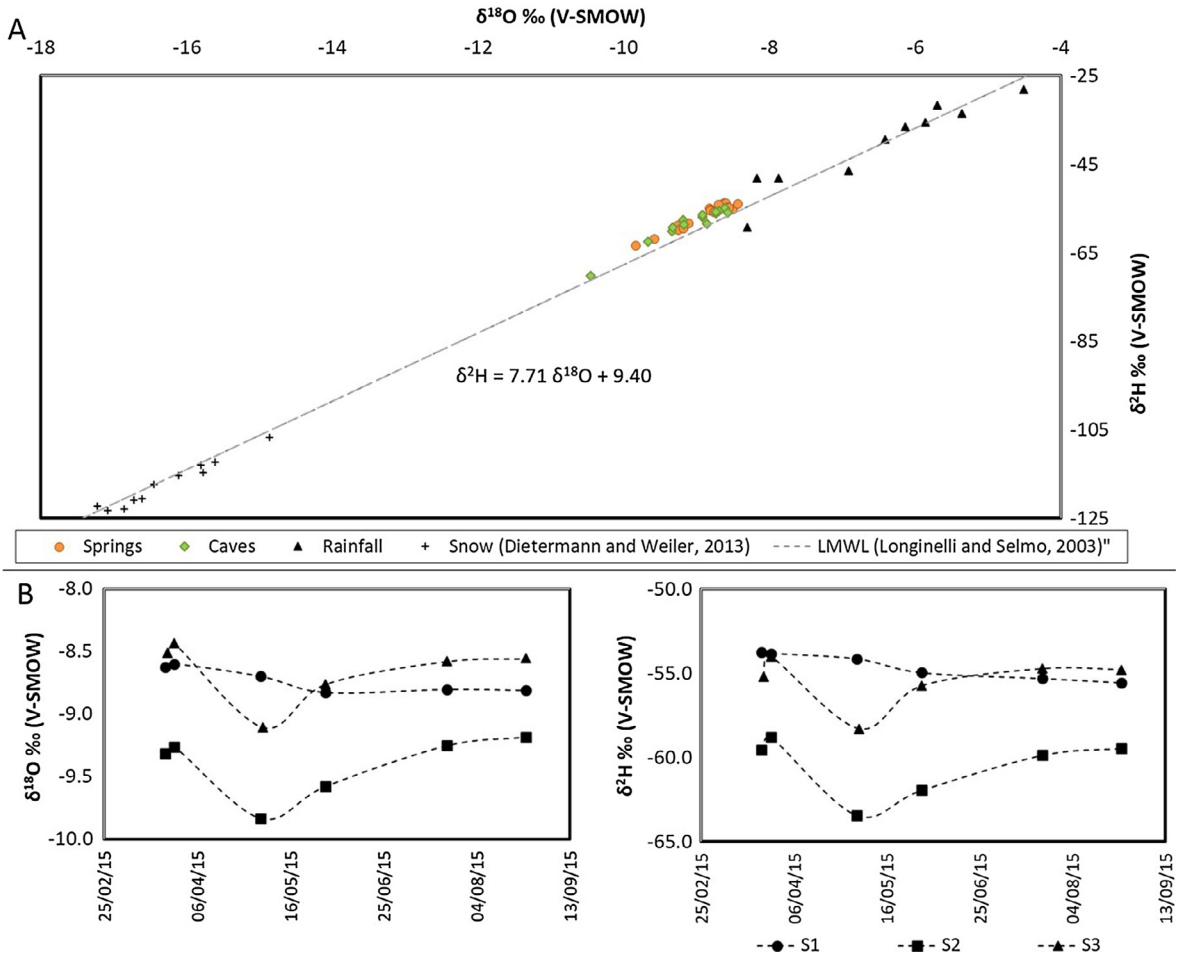

Fig. 9. (A) Stable isotope signature of rain, cave waters and springs; the equation describes the Local Meteoric Water Line (LMWL) for North Italian waters (Longinelli and Selmo, 2003). Snow composition measured by Dietermann and Weiler (2013) in the Taschinasbach catchment area (eastern Alps, Switzerland) is reported for comparison; (B) stable isotope values measured over time at the three springs. Details on the sampling rounds and measured values are in the Supplementary Material.

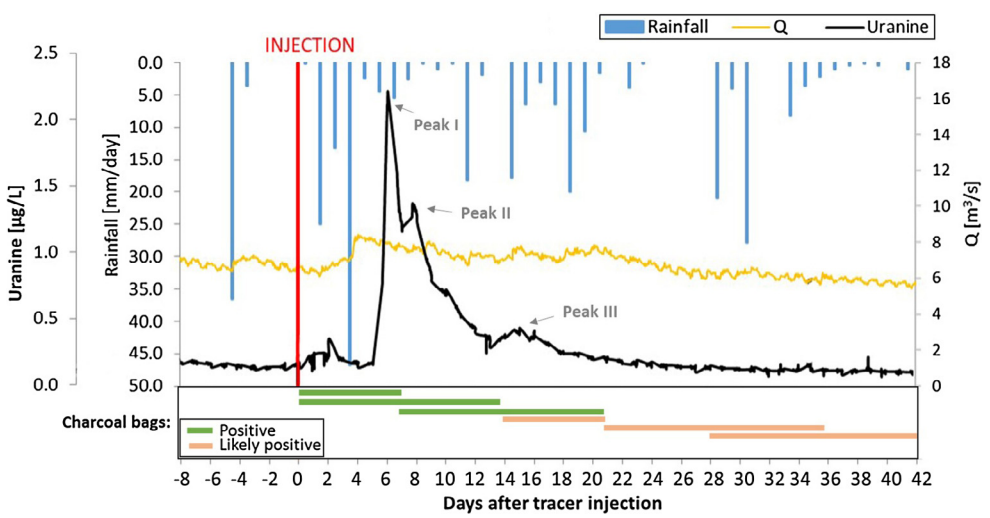

Fig. 10. Breakthrough curve of Uranine at S2 spring (daily rainfall and hourly measurements for Q and tracer concentration).

turbed signals were observed at S1 and S3 springs for all the three tracers injected. Some examples of disturbed fluorometer signals are reported in the Supplemental Material. The overall lack of clear and reliable tracer-test outcomes is either attributable to anthropogenic noise (e.g. domestic wastewater from washing machines), to the huge dilution potential of the aquifer system, to missing connectivity between the tested caves and springs, or to the insufficient length of the observation period (70–90 days).

5. Discussion

The S1, S2, and S3 springs are located on a permeability threshold, which puts the Mesozoic limestones of the Cansiglio massif in contact with the impervious flysh units to the East.

The altitude of these springs is about 150 m lower than the S4, which appears to drain the dolomitic carbonate rocks on the western slope of the Meschio river based on the geometry of the explored conduits, the higher Mg^{2+} content, and no detection of tracers in the spring. Thus, the S1, S2 and S3 appear to be only large groundwater outlets of the Cansiglio-Monte Cavallo aquifer system.

The three springs show a distinct hydrological and geochemical behavior: S3 is a typical interconnected circulation system, reacting in a pronounced way to major infiltration events (with peaks of almost 18 m^3/s, falling to completely dry conditions at the end of drought periods). It shows its most significant responses to recharge during the snowmelt hydroperiod and less important during the heavy rainfall hydroperiod. Snowmelt waters contribute directly to S3 recharge, as indicated by the negative peak in water stable isotopes detected during the snowmelt hydroperiod. EC and temperature decrease significantly after the main recharge events during both the snowmelt and rainfall hydroperiods. This indicates direct flow contributions from the surface to the spring. The higher concentration in Mg^{2+} detected in S3 with respect to S2 and S1 indicates part of its drainage basin to include dolomitic rocks, mainly present at depth (lower part of the carbonate succession) and in the northeastern part of the study area (close to Piancavallo). Based on this last evidence, the recharge area of the spring almost surely comprises part of the Piancavallo area (Fig. 11). Also, the exploration of the S3 spring up to 165 m bsl demonstrates the presence of a deep and extensive saturated network of conduits feeding the spring, which could intercept the dolomitic rocks of the deep succession.

S2 spring is another example of interconnected circulation system, with clear evidence of flow along well-developed conduits. S2 has less pronounced flow rate variations with respect to S1 and S3, and has the highest average flow rate, representing the main outflow of the karst aquifer. One of the most striking and surprising differences with the other two main springs is water temperature, S2 being 1–2 °C colder. This would suggest its recharging waters to come, at least in part, from higher (thus colder) altitudes. The higher altitude of the recharging waters is confirmed by the stable isotope values, which are lower for S2 compared to the other two springs. Considering the average N-Italian isotopic altitude gradient of 0.21‰ per 100 m, a significant part of S2 waters has to come from areas located at least 350 m higher than the drainage areas of the other two springs. This leads us to conclude that S2′s drainage basin comprises part of the Piancavallo mountain chain and/or the Mount Pizzoc area (Fig. 11). On the other hand, based on dye trace results, S2 surely drains also the Cansiglio plateau (where the C1 cave is located). S2 appears thus to drain a large recharge basin that covers a wide range of altitudes. This would explain the constantly high flow rate of the spring.

S1 spring appears to be fed by a less karstified section of the aquifer with respect to S2 and S3, behaving halfway between an interconnected circulation system and a dispersive circulation system, with no (or poorly karstified) main conduits. This is supported by the rather low variability in water stable isotopes and the contents in Lanthanoids typical of waters in prolonged contact with carbonate rocks. In particular, the contents in Lanthanoids indicate a more pronounced fingerprint in S1 waters and a more subdued one in S3, indicating the latter to have a shorter water-rock interaction. Also, S1 shows more irregular flow rate changes after the main recharge events with respect to the other two springs: this suggests the spring to be recharged by dispersive rather than preferential flowpaths. The slight increase in EC and T after the main recharge events indicates a slight piston flow, in which resident waters are pushed out from the aquifer by transfer of hydraulic pressure. Based on the tracer experiments carried out by Vincenzi et al. (2011) that showed a connection with the C2 cave, the S1 spring probably drains a relatively low karstified sector of the massif that extends from the spring itself to the Cansiglio plateau (Fig. 11).

All the hypothesized drainage areas (Fig. 11) are linked to the springs along directions that are consistent with the main flow directions identified by the lineament analysis of the karst massif (i.e. the ENE-WSW and NW-SE directions).

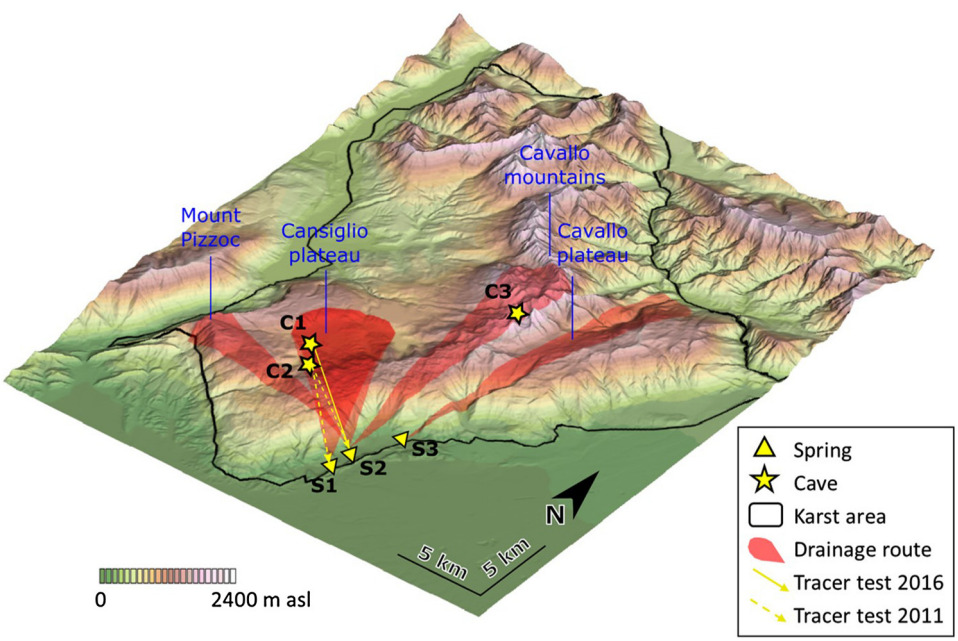

Fig. 11. 3D map of the Cansiglio-Monte Cavallo karst area. The main drainage routes defined in this study are highlighted in red. The yellow arrows show the cave-spring connections ascertained by the tracer test of Vincenzi et al. (2011 – dashed arrows) and the current tracer test (2016 – solid line).

During low-flow conditions, the three springs drain their recharge areas independently, as shown by their geochemical differences. The drainage areas of S1 and S2 must be partially overlapped since the tracing experiment of Vincenzi et al. (2011), performed in low-flow conditions, allowed demonstrating a connection of the C2 cave with both springs. During high-flow periods, the different compartments in the aquifer are more interconnected, as demonstrated by the homogenization of major ion composition in the three springs, and eventually neo-infiltrating water is responsible for the main imprint of the spring waters, as suggested by the flattening of the curve of Lanthanoids after the main recharge events.

Although our dye tracing experiment did not deliver definitive results, a direct connection between C1 cave and S2 spring was confirmed, with fast arrival times and an unexpected high recovery rate (75%). The higher groundwater flow velocity and recovery rate in comparison with the ones assessed by Vincenzi et al. (2011) suggest that the aquifer system is more "active" (likely more interconnected) during the recharge period (as in the current tracer test) with respect to the dry period (as in the test performed by Vincenzi et al.). This last observation is consistent with the research of Devoti et al. (2015) that observed the karst massif to respond very actively (i.e. quickly and impulsively) to the main recharge events, in terms of hydrologically induced slope deformation. The use of both Aminorhodamine-G and Tinopal CBS-X, even with rather high tracer amounts injected, has been inconclusive.

6. Conclusions

The multidisciplinary research has allowed gathering an ample set of data, shedding light on a part of the aquifer system, but still leaves room for speculations of unknowns. Based on all the data, the Cansiglio-Monte Cavallo karst area can be defined as an unusual karst aquifer system with an interconnected drainage network. The karst aquifer system shows an intricate geometry that is due to the structural complexity of the investigated area and to the peculiar speleogenetic evolution. It is drained by only three main outflows (excluding the S4 spring) that can be fitted in different underground karst conceptual models even if very closely spaced. The three springs respond differently to recharge events (controlled by either rainfall or snowmelt), despite the fact that their general chemistry suggests that they drain more or less the same kinds of rocks. The most surprising fact is that the difference in chemistry is less pronounced during high flow conditions with respect to low flow, suggesting the conduit and karstified fracture systems being more interconnected, and thus the system more active, under these conditions.

From a methodological viewpoint, the general lack of compelling tracer test outcomes suggests that the use of dyes in the context of extensive alpine karst aquifers drained by large springs and affected by anthropogenic impacts (e.g. wastewater from houses or ski resorts) may turn out to be ineffective in some cases, even when performed in ideal conditions (i.e. at the beginning of a recharge season, active flow at the injection point, large amounts of tracer injected), whereas an adequate hydrodynamic, hydrogeochemical and isotopic monitoring of caves and springs can provide much more valuable information on the system behavior.

Acknowledgements

This complex hydrogeological study would not have been possible without the help of the many cavers operating in the Cansiglio area, especially about 40 members of the Unione Speleologica Pordenonese CAI, Gruppo Speleologico CAI Vittorio Veneto, Gruppo Speleologico Sacile, Gruppo Grotte "Solve" CAI Belluno, and Gruppo Speleologico Ferrarese. We acknowledge the Municipalities of Caneva, Polcenigo and Budoia, the local restaurants "La Trota Blu" and "Pizzeria da Genio", and the keeper of the Polcenigo aqueduct for allowing the monitoring activities and the installation of instruments. We also acknowledge Prof. Carla Braitenberg (University of Trieste) for providing one of the Diver transducers, the divers Alberto Casagrande and Denis Zanette for the recovery of underwater instruments and Luca Tedesco for the support during fieldwork. Finally we thank Lukas Plan and an anonymous reviewer for their useful comments and corrections.

Appendix A. Supplementary data

Supplementary data associated with this article can be found, in the online version, at https://doi.org/10.1016/j.jhydrol.2017.11.040.

References

Ballesteros, D., Malard, A., Jeannin, P.-Y., Jiménez-Sanchez, M., Garcia-Sansegundo, Meléndez-Asensio, M., Sendra, G., 2015. KARSYS hydrogeological 3D modeling of alpine karst aquifers developed in geologically complex areas: Picos de Europa National Park (Spain). Environ. Earth Sci. 74, 7699–7714.

Cancian, G., Ghetti, S., Semenza, E., 1985. Aspetti geologici dell'Altipiano del Cansiglio. Lavori della Società Veneta di Scienze Naturali, suppl. 10, 79-90. In Italian.

Cavallin, A., 1979. Assetto strutturale del Massiccio Cansiglio – Cavallo, Prealpi Carniche Occ. Atti del 2° Convegno di Studi sul Territorio della provincia di Pordenone (Piancavallo, Oct. 19-20, 1979), pp. 15–32 (In Italian).

Civita, M., Cucchi, F., Eusebio, A., Garavoglia, S., Maranzana, F., Vigna, B., 1995. The Timavo hydrogeologic system: an important reservoir of supplementary water resources to be reclaimed and protected. Acta Carsol. 24, 169–186.

Cucchi, F., Finocchiaro, F., 2017. Karst Landforms in Friuli Venezia Giulia: From Alpine to Coastal Karst. In: Soldati, M., Marchetti, M. (Eds.), Landscapes and Landforms of Italy. Springer International Publishing, Cham, pp. 147–156.

Cucchi, F., Forti, P., Giaconi, M., Giorgetti, F., 1999. Note idrogeologiche sulle sorgenti del Fiume Livenza. Atti Giornata Mondiale dell'Acqua, Roma 1998, Pubblicazione CNR-GNDCI 1831,pp. 51–60 (In Italian).

Devoti, R., Zuliani, D., Braitenberg, C., Fabris, P., Grillo, B., 2015. Hydrologically induced slope deformations detected by GPS and clinometric surveys in the Cansiglio Plateau, southern Alps. Earth Planet. Sci. Lett. 419, 134–142.

Dietermann, N., Weiler, M., 2013. Spatial distribution of stable water isotopes in alpine snow cover. Hydrol. Earth Syst. Sci. 17 (7), 2657–2668.

Goldscheider, N., Neukum, C., 2010. Fold and fault control on the drainage pattern of a double-karst-aquifer system, Winterstaude, Austrian Alps. Acta Carsol. 39 (2), 173–186.

Grillo, B., 2007. Contributo alle conoscenze idrogeologiche dell'Altopiano del Cansiglio. Atti e Memorie della Commissione Grotte "E. Boegan". Trieste 41, 5–15. In Italian.

Grillo, B., Braitenberg, C., Devoti, R., Nagy, I., 2011. The study of karstic aquifers by geodetic measurements in Bus de la Genziana station-Cansiglio Plateau (Northeastern Italy). Acta Carsol. 40 (1), 161–173.

Hartmann, A., Goldscheider, N., Wagener, T., Lange, J., Weiler, M., 2014. Karst water resources in a changing world: review of hydrological modeling approaches. Rev. Geophys. 52, 218–242.

Jeannin, P.Y., Eichenberger, U., Sinreich, M., Vouillamoz, J., Malard, A., Weber, E., 2013. KARSYS: a pragmatic approach to karst hydrogeological system conceptualisation. Assessment of groundwater reserves and resources in Switzerland. Environ. Earth Sci. 69 (3), 999–1013.

Johannesson, K.H., Stetzenbach, K.J., Hodge, V.F., Kreamer, D.K., Zhou, X., 1997a. Delineation of ground-water flow system in the Southern Great Basin using aqueous rare earth element distribution. Groundwater 35 (5), 807–819.

Johannesson, K.H., Stetzenbach, K.J., Hodge, V.F., 1997b. Rare earth elements as geochemical tracers of regional groundwater mixing. Geochim. Cosmochim. Acta 61 (17), 3605–3618.

Kuebeck, C., Maloszewski, P., Bensichke, R., 2013. Determination of the conduit structure in a karst aquifer based on tracer data-Lurbach system, Austria. Hydrol. Process. 27, 225–235.

Lauber, U., Goldscheider, N., 2014. Use of artificial and natural tracers to assess groundwater transit-time distribution and flow systems in a high-alpine karst system (Wetterstein Mountains, Germany). Hydrogeol. J. 22 (8), 1807–1824.

Lee, S., Lee, D., Kim, Y., Chae, B., Kim, W., Woo, N., 2003. Rare earth elements as indicators of groundwater environment changes in a fractured rock system: evidence from fracture-filling calcite. Appl. Geochem. 18, 135–143.

Liu, J., Yang, H., Gosling, S.N., Kummu, M., Flörke, M., Pfister, S., Hanasaki, N., Wada, Y., Zhang, X., Zheng, C., Alcamo, J., Oki, T., 2017. Water scarcity assessments in the past, present, and future. Earth's Future 5, 545–559.

Longinelli, A., Selmo, E., 2003. Isotopic composition of precipitation in Italy: a first overall map. J. Hydrol. 270 (1), 75–88.

Luo, M., Chen, Z., Zhou, H., Jakada, H., Zhang, L., Han, Z., Shi, T., 2016. Identifying structure and function of karst aquifer system using multiple field methods in karst trough valley area, South China. Environ. Earth Sci. 75 (9), 824. https://doi.org/10.1007/s12665-016-5630-5.

Marín, A.I., Andreo, B., 2015. Vulnerability to contamination of Karst Aquifers. In: Stevanović, Z. (Ed.), Karst Aquifers—characterization and engineering, professional practice in Earth Sciences. Springer, Berlin, pp. 251–266.

Meinzer, O.E., 1923. Outline of ground-water hydrology. US Geol. Surv. Water Supply Pap. 494, 5.

Nagarajan, R., Madhavaraju, J., Armstrong-Altrin, J.S., Nagendra, R., 2011. Geochemistry of Neoproterozoic limestones of the Shahabad Formation, Bhima Basin, Karnataka, southern India. Geosci. J. 15 (1), 9–25.

Panagopoulos, G., Lambrakis, N., 2006. The contribution of time series analysis to the study of the hydrodynamic characteristics of the karst systems: application on two typical karst aquifers of Greece (Trifilia, Almyros Crete). J. Hydrol. 329 (3), 368–376.

Perrin, J., Luetscher, M., 2008. Inference of the structure of karst conduits using quantitative tracer tests and geological information: example of the Swiss Jura. Hydrogeol. J. 16 (5), 951–967.

Piper, D.Z., 1974. Rare-Earth elements in the SediCycle: a summary. Chem. Geol. 14, 285–304.

Plan, L., Kuschnig, G., Stadler, H., 2010. Kläffer spring – the major water supply spring of the Vienna water supply (Austria). In: Kresic, N., Stevanovic, Z. (Eds.), Groundwater Hydrology of Springs. Engineering, Theory, Management, and Sustainability. Butterworth-Heinemann, Burlington, pp. 411–427.

Ravbar, N., Goldscheider, N., 2009. Comparative application of four methods of groundwater vulnerability mapping in a Slovene karst catchment. Hydrogeol. J. 17, 725–733.

Ravbar, N., Engelhardt, I., Goldscheider, N., 2011. Anomalous behaviour of specific electrical conductivity at a karst spring induced by variable catchment boundaries: the case of the Podstenjšek spring, Slovenia. Hydrol. Processes 25 (13), 2130–2140.

Schnegg, P.A., Costa, R., 2003. Tracer tests made easier with field fluorometers. Bull. d'Hydrogeol. 20, 89–91.

Stumpp, C., Żurek, A.J., Wachniew, P., Gargini, A., Gemitzi, A., Filippini, M., Witczak, S., 2016. A decision tree tool supporting the assessment of groundwater vulnerability. Environ. Earth Sci. 75 (13), 1057.

Terzić, J., Stroj, A., Frangen, T., 2012. Hydrogeological investigation of karst system properties by common use of diverse methods: a case study of Lička Jesenica springs in Dinaric karst of Croatia. Hydrol. Process. 26 (21), 3302–3311.

Turk, J., Malard, A., Jeannin, P.-Y., Petrič, M., Gabrovšek, F., Ravbar, N., Vouillamoz, J., Slabe, T., Sordet, V., 2015. Hydrogeological characterization of groundwater storage and drainage in an alpine karst aquifer (the Kanin massif, Julian Alps). Hydrol. Process. 29 (8), 1986–1998.

Vincenzi, V., Riva, A., Rossetti, S., 2011. Towards a better knowledge of Cansiglio karst system (Italy): results of the first successful groundwater tracer test. Acta Carsol. 40 (1), 147–159.

B. Vigna B., 2010. Gli acquiferi carsici. Dispense didattiche della Società Speleologica Italiana, Erga edizioni, Genova, pp. 1–48 (In Italian).

Vigna, B., Banzato, C., 2015. The hydrogeology of high-mountain carbonate areas: an example of some Alpine systems in southern Piedmont (Italy). Environ. Earth Sci. 74 (1), 267–280.

Wachniew, P., Zurek, A.J., Stumpp, C., Gemitzi, A., Gargini, A., Filippini, M., Rozanski, K., Meeks, J., Kværner, J., Witczak, S., 2016. Toward operational methods for the assessment of intrinsic groundwater vulnerability: a review. Crit. Rev. Environ. Sci. Technol. 46 (9), 827–884.

White, W.B., 2002. Karst hydrology: recent developments and open questions. Eng. Geol. 65, 85–105.

Zini, L., Calligaris, C., Treu, F., Zavagno, E., Iervolino, D., Lippi, F., 2013. Groundwater sustainability in the Friuli Plain. AQUA Mundi 4, 41–54.

Zini, L., Calligaris, C., Zavagno, E., 2014. Classical karst hydrodynamics: a shared aquifer within Italy and Slovenia. Proc. Int. Assoc. Hydrol. Sci. 364, 499–504.